N-k Security Assessment With Quantum Annealing

Jochen Lorenz Cremer, *Member, IEEE*

***Abstract*—Suppose one is interested in identifying the weakest link of the electrical system at 3 simultaneous faults caused by an extreme weather event. Current techniques cannot identify this; however, knowing such information can help reinforce the system at the weakest link to increase system security. Current techniques typically apply a forward process to the security assessment: assign a contingency list, study its impact, analyse the list to obtain a shortlist, and improve the system. However, this process does not scale well to the number of contingencies, specifically, when one is interested in the combination of k faults, as the process needs to run once per combination. This paper proposes a new backwards process using quantum effects from quantum annealing (QA). Our proposal formulates a quadratic optimisation to find the worst-case N-k contingency using disjunctive power transfer distribution factors. Then, we use a quantum annealer and propose a search algorithm to solve the problem, using the distribution of solutions to obtain the shortlist of contingencies. We propose a meta-heuristic to make the approach feasible on quantum computers with limited qubits. The case studies focus on the IEEE 118-bus system, showing a 200× speed-up for 50 faults compared to exhaustive search. The case study extrapolates to the 2383wp system, showing the approach scales well to larger power systems; however, the current quantum hardware limits the number of single faults to consider to around 50. Case studies demonstrate weak lines can be identified for reinforcement by analysing the QA solution distribution, potentially improving system security for multiple N-k faults.**

***Index Terms*—Security assessment, extreme events, power system resilience, quantum computing.**

NOMENCLATURE

Indices

0	Initial.
$\mathcal{L}, l, \hat{l}, \check{l}$	Line.
$b, \tilde{b}$	Bus.
c	Combination of two lines.
d	Fault.
d^*	Worst-case contingency.
i	Sample of two-line combinations.

Sets

$\hat{\Omega}^Y$	Unique solutions from QA.
Ω^B	Buses of the system.
Ω^L	Lines of the system.
Ω^Y	Shortlist of contingencies.
$\Omega^{\hat{L}}$	Set of lines in outage.
$\Omega_d^{\hat{L}}$	Lines in outage at fault d.
Ω^{CL}	Two-line combinations that are too closev.
Ω^C	Combinations that correspond to faults where two lines are simultaneously in outage.
Ω_i^C	Subset i of two-line combinations in outage $\Omega_i^C \subset \Omega^C$.
Ω^D	Set of contingencies.
Ω^{FL}	Two-line combinations that are sufficiently far away.

Parameters

$\bar{\rho}$	Threshold to include solutions d in contingency list.
χ_l	Reactance of line l.
δ^B	Threshold on minimal shortest path.
$\delta_{l,\hat{l}}$	Minimal shortest path between lines l and line $\hat{l}$.
$\mathcal{F}_l$	Matrix summarizing the diagonal slices at line l of tensors F, G, and H.
$\mathcal{G}_c$	Matrix of the mean off-diagonal symmetric entries of G, computed for the two lines associated with c.
$\mathcal{H}_{l,c}$	Matrix of the mean off-diagonal symmetric entries of H_l, computed for the two lines associated with c.
$\mathcal{I}$	Identity matrix.
$\mathcal{P}_{\mathcal{L}}^A$	Pre-fault power flow in line $\mathcal{L}$.
$\mathcal{P}_{l,\mathcal{L}}^B$	Change in power flow on $\mathcal{L}$ due to the outage of l.
$\mathcal{P}_{c,\mathcal{L}}^C$	Change in power flow on line $\mathcal{L}$ due to the outage of the two lines associated with the combination c.
$\mathcal{P}_{l,c,\mathcal{L}}^D$	Change in power flow on line $\mathcal{L}$ due to outage of three lines: line l and two lines associated with c.
$\mathcal{Q}$	Real-valued upper triangular matrix for QUBO.
$\tilde{B}$	Approximation of susceptance matrix.
A	Incidence matrix.
b_l^f	'From bus' of line l.
b_l^t	'To bus' of line l.
B_{br}	Line reactance matrix.
D	Matrix representing the change in the susceptance matrix due to fault d.
e_i	Standard basis vector where ith element is one.
E_l	Reference matrix to expand with the second Neumann Series around line l.
f^0	Pre-fault power flow.
$f_{\mathcal{L}}^B$	Limit of the power flow over line $\mathcal{L}$.
$H_{l,\hat{l},\check{l}}$	Matrix of the line outages l, $\hat{l}$ and $\check{l}$ that contributes to the inverse of the approximate susceptance matrix.

Received 26 January 2025; revised 25 July 2025; accepted 4 October 2025. Date of publication 7 October 2025; date of current version 23 February 2026. This work was supported in part by Dutch Research Council, Veni Talent Program, under Grant 19161, and in part by Delft AI Initiative Program. Paper no. TPWRS-00177-2025.

The author is with the Department of Electrical Sustainable Energy, Delft University of Technology 2628 CD Delft, The Netherlands, and also with the Centre for Energy, Austrian Institute of Technology 1210 Vienna, Austria (e-mail: j.l.cremer@tudelft.nl).

Color versions of one or more figures in this article are available at https://doi.org/10.1109/TPWRS.2025.3618916.

Digital Object Identifier 10.1109/TPWRS.2025.3618916

J_l	Reference matrix to expand with the first Neumann Series around line l.
k	Number of simultaneous faults.
N	Elements in the system.
p	Vector of power injections.
Q	Number of qubits.
R_l	Perturbation matrix in the second Neumann expansion around E_l, corresponding to line l.
T_l	Component of the perturbation matrix in the first Neumann expansion around J_l, corresponding to l.
U	Matrix of left singular vectors of D.
U_l	Rank-one diagonal matrix with -1 at the 'to bus' b_l^t of line l.
V	Matrix of right singular vectors of D.
V_l	Rank-one diagonal matrix with $-\frac{1}{\chi_l}$ at the 'from bus' b_l^f of line l.
B	Susceptance matrix.
F_l	Matrix of the line outage l that contributes to the inverse of the approximate susceptance matrix.
$G_{l,\hat{l}}$	Matrix of the line outages l and $\hat{l}$ that contributes to the inverse of the approximate susceptance matrix.
$C_1, C_2\ C_3$	Scalar weights for terms in the objective function.

Variables

$\lambda, \lambda^{\pm}$	Maximal violation of line loading constraints.
$\lambda_{\mathcal{L},d}$	Loading on line $\mathcal{L}$ under solution d computed by approximate PTDFs.
$\overline{\lambda}_{\mathcal{L},d}$	Loading on line $\mathcal{L}$ under solution d computed by accurate PTDFs.
ρ_d	Share of runs producing solution d.
$f_{\mathcal{L}}$	Power flow over line $\mathcal{L}$.
u	The uth most loaded line in the system.
y_l	Binary variable indicating if line l is in outage.
z_c	Binary variable indicating if the two lines corresponding to combination c are in outage.

Others

$h(\cdot)$	Bijective function assigning a two-line combination.
$o(\cdot)$	Function mapping u to the line $\mathcal{L}$ with the uth largest line flow.
$R(\cdot)$	Function rounding down to closest integer that is smaller.

I. Introduction

INTEGRATING renewable energy into the grid and the increasing electricity demand cause new operating patterns and possible fault conditions for which the system was not designed. Operating the system closer to its limits, experiencing more extreme weather events, and ageing transmission equipment may lead to increased N-k failures in the future [1]. Currently, cascading failures may lead to power blackouts, where one failure leads to another failure in cascades (such as considered in [2]). When assessing the system to the impact of a cascading failure, often the first failure is simulated; subsequently, the next failure is simulated and assessed, e.g. k simulations are needed per cascade. Therefore, analysing cascading with k-failures is computationally hard as exploring all combinations requires consecutive analysis [3]. [2] provides an algorithm to identify a shortlist of k-cascading failures in linear computational time. In contrast to cascading failures, simultaneous, independently occurring faults are rare. However, when a common mode is present, multiple k-failures may also occur (common mode failures). These k-failures that have a common dependency may increase in the future due to an increase in extreme events as a common mode (see Fig. 1). In the future, extreme windstorms, wildfires, or floods can cause simultaneous and multiple (k) failures of N transmission equipment. This paper focuses on common mode failures, aiming to screen many k-contingency combinations, and assumes that assessing security for one k-fault combination requires one computational step.

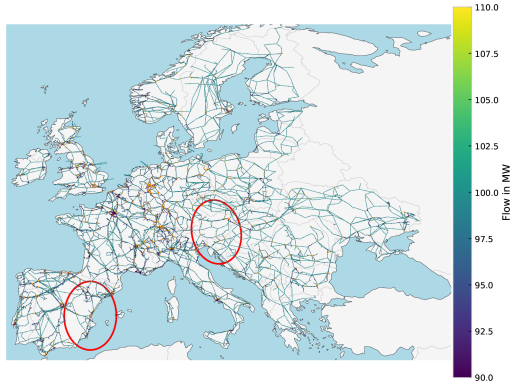

Fig. 1. The use case studies k-failures originating from multiple extreme events such as two floods around Vienna and Valencia (2024). The red circles show the local impact of those floods that may locally lead to k-failures. This initial work may help assess France's system security in response to these events, for example. Figure generated with data from [41].

Considering the risks of k-failures (as [4], [5]) has the potential to improve system design [6] and planning [7], [8], however, new tools and methods are needed to realise this potential [9]. Upgrading the tooling for planning and operating these systems becomes critical so that system operators can ensure the security of the supply, also during these extreme scenarios. Assessing system properties such as security, reliability, or resilience against all possible N-k fault combinations is needed for a wide variety of operating conditions, but it is challenging with current methods. Most available methods require individual computational steps for each combination of faults to assess the system's properties. This requirement is beyond the computing capabilities currently available. Calculating post-fault power flows of various combinations of faults (N-k with $k > 1$) requires either a large number of post-fault AC power flows [10], applying the DC approximation, heuristics [11], or Generalised Line Outage Distribution Factors (GLODF) [12]. LODFs are a matrix for a fault that, when multiplied by the pre-fault line flows, provides the post-fault line flow [13]. GLODF generalises this matrix to the combination of multiple line failures. The Power Transfer Distribution Factors (PTDF) multiplied by the power injections at all buses provide the power flow over the lines in the

network. PTDFs can also be formulated for a network with faults; however, each fault condition requires a separate PTDF matrix.

Several approaches can identify the worst-case contingency, for example, by exhaustively comparing all fault combinations and analysing whether their post-fault power flows surpass thermal line ratings, then ranking these to identify the worst-case. [14] directly detects the worst-case k-fault using nonlinear optimisation. The approach is limited in system size and cannot guarantee global optimality. [15] proposes an algorithm using sensitivities to efficiently assess $k = 2$ contingencies. [16] formulates the N-k problem as a bilevel mixed integer nonlinear optimisation (MINLP) modelling a combinatorial problem and fixing continuous variables. [11] considers the upper-level problem as the combination of line outages, and the lower-level problem models the operation. Their proposed genetic algorithm can detect critical contingencies; however, the approach may be slow for larger systems. Over the years, these approaches to detecting worst-case contingencies advanced; however, these approaches are not focused on identifying a set of critical fault combinations as the primary target that goes beyond the worst-case. Obtaining a distribution of solutions that may include the worst-case provides further insights, e.g. which line to reinforce to improve security for multiple k-failures.

Approaches that identify a critical set, a shortlist of fault combinations, often approximate the properties of the system to keep computational times practical. Various approaches create these shortlists (also called contingency lists), such as Monte Carlo (MC) type sampling, heuristics, or the N-1 criterion. For example, [17] uses the electrical distance to identify vulnerable $N - 3$ fault combinations and avoids solving AC power flows. MC-type sampling may consider the statistical dependency of faults to create shortlists, as some fault combinations are more likely than others [18]. Other approaches identify high-risk contingencies [19], predict with machine learning [20], [21], rank contingencies [22], or apply probabilistic security [23]. [19] performs time-domain simulations after each fault, subsequently selecting a new fault, such as in a linear search. The time-domain assessments provide high accuracy; however, approaches that apply linear search may miss some insecure k-combinations of faults, especially if these originate from a common mode such as an extreme weather event. [22] uses the risk and the loss of load to rank worst-case contingencies. However, one optimisation is required per contingency scenario to identify all severities beyond the worst-case, leading to very high computational times in large systems. [23] proposes a probabilistic assessment of the contingencies where the severities are calculated per contingency scenario. There, each scenario requires an individual computational step. Identifying multiple N-k contingencies by applying existing methods remains challenging for large systems and $k > 1$, as each combination of faults requires one computational step, and the number of steps 'explodes' combinatorially with k and the system size. For example, applying LODFs requires matrix inversions for each fault combination ($k > 1$). Recently, polynomial distribution factors have shown benefits when computing system properties such as probabilistic security for N-k failure combinations [24]. These polynomial distribution factors approximate the PTDFs for combinations of line faults.

Securing against N-k contingencies goes beyond assessing an operating condition against the shortlist of contingencies. The Security Constrained Optimal Power Flow (SCOPF) problem can consider k-failures, ensuring a probabilistic level of security. [25] shows the operation is sensitive to common-mode probabilities of extreme events. LODFs can ensure security considering preventive control, whereas robust optimisation can also consider corrective control securing against k-contingencies [26]. Nonetheless, including a large number of combinations of k-faults in larger power systems may lead to very large optimisations that are hard to solve. In response, combining deep learning with optimisation has been proposed to consider a vast number of contingency combinations [8]. However, these methods currently do not aim to reinforce a single line to improve against multiple N-k contingencies, which can be of interest. Aiming at reinforcing the network, one could combine the grid expansion planning problem with N-k SCOPF, leading to a potentially impractical approach as it would include binary variables and many constraints for combinations of k-faults. The shared weakness of most aforementioned approaches aiming at assessing or securing against k-failures is limiting the number of scenarios and conditions that are assessed, leaving a residual risk of the conditions not being shortlisted, which endangers the security of supply. Sequential or parallel processing cannot overcome this limitation in a principled way, which leads this paper to explore quantum computing.

Approaches based on quantum computers are promising in addressing this limitation of sequential processing faults by evaluating all N-k fault scenarios in a single computing step. More broadly, quantum computing (QC) may address some challenges related to power system computing [27], [28]. Two types of QC are gate-based QC and quantum annealing (QA). Gate-based QC can be used for a broad range of problems, whereas QA is used primarily for optimisation problems. [29], [30] develop a theory for Gate-based QC to solve power flow problems. Gate-based QC with the Harrow-Hassidim-Lloyd algorithm was investigated for the N-k security assessment [31]. [31] mentioned QC-based methods based on LODFs that can compute N-k power flows and reduced computations. More broadly, gate-based QC was applied to the reliability of the power system for distribution systems [32] and to the assessment of risks in an MC-type approach [33]. [32] shows benefits when N-1 security reliability assessments replace MC sampling to approximate a function of the system property. However, gate-based QC is only available with a few qubits, and industrial-level realisation may take time. Recently, [34] has approached the reliability assessment of the system using quantum computing theory and iteratively estimating the quantum amplitude. Such iterative heuristics include the current available QC hardware in power systems heuristics. QA is a heuristic algorithm that solves quadratic unconstrained binary optimisation (QUBO) problems, can be combined with classic solvers as hybrids [35], and is combined with meta-heuristics for hybrid methods if too many variables exist, e.g. tabu search that DWave deploys. QA is

already available in QC with qubits on the order of 10,000, opening up the opportunity to develop approaches for practical use. Recently, [36], [37] investigated QA for AC power flows, reformulating the problem through discretisation and [38] for DC power flow. Unlike digital (and simulated) annealing on classical computers, QA holds a potential advantage in using quantum effects (quantum tunnelling) to reach solutions which may be exploited for power system use cases.

Formulating QA-solvable power system problems (such as QUBO [39]) requires considering QA errors, assessing end-to-end computational complexity, and comparing them with heuristic baselines. The end-to-end complexity in QA refers to computational complexity that includes both classical pre-processing (embedding) and quantum processing (annealing time) [40]. QA can solve QUBO problems; however, challenges also exist. The QA hardware has a specific connectivity of qubits, allowing only solving a subclass of QUBOs. QA has errors and may find different local optima across runs and not necessarily the global optima. This issue is often addressed by multiple runs of QA or varying parameters (like annealing time), and analysing the distribution of solutions to increase reliability in the solution's optimality.

This research aims at tailored heuristics to solve the N-k security assessment problem, combining QA solving QUBOs and a Neumann series approximation for PTDFs. This paper proposes formulating the N-k security assessment as a constrained, disjunctive mixed-integer nonlinear optimisation. Then, the paper proposes a quadratic reformulation of line flow limits leading to multiple QUBOs that can be solved with QA or digital annealing. The proposed approach solves a series of QUBOs to approach the N-k security assessment. The proposed approaches minimise overall errors from QA and the series approximation. Then, this paper proposes a meta-heuristic, a variation of the proposed formulation that makes the approach feasible using a finite, limited number of qubits by adapting an MC-type approach. Finally, this paper exploits the probabilistic nature of annealing (here the quantum effects) so that the distribution of solutions suggests line reinforcements of weak lines. The three contributions are

1) quadratic formulation of N-k security assessment problem as worst-case optimisation using disjunctive PTDFs. This formulation can be solved by QUBOs on QA, and the distribution provides the set of insecure contingencies, representing a novel backwards process to security assessment.
2) search algorithm that iteratively applies QA to the QUBO set to solve the N-k security assessment. This algorithm can approach the N-k security assessment problem given many qubits.
3) customised meta-heuristic algorithms using partitioning and an MC-type approach that improves scaling of these algorithms on limited QC hardware of finite qubits.

Case studies on the IEEE 118-bus system investigate the error of the disjunctive N-k security assessment. Errors increase with the proximity of faults. One use case determines the contingency lists from the output distribution of the QA-based approach, and the other use case identifies lines to reinforce to make the system more secure against k-failures. The final case studies assess the computing times compared with a state-of-the-art solver, GUROBI, and conventional forward security assessment. We also test the meta-heuristic search approach to see what is currently possible with existing annealers.

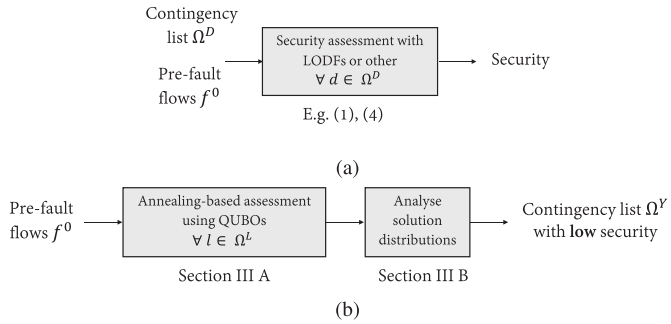

Fig. 2. Conventional SA (a) requires many sequential computations for a large set of contingencies Ω^D that include combinations of k faults. Proposed annealing-based SA (b) outputs the set of contingencies that are low in security, leading to overloads in lines Ω^L. Proposed (b) requires fewer computations than (a) as $|\Omega^L| \ll |\Omega^D|$ for N-k faults where $k > 1$.

II. Disjunctive N-k Security Assessment

The $PTDF_d$ compute the line flows

$$f_{\mathcal{L}} = PTDF_d \times p \qquad \forall \mathcal{L} \in \Omega^L \tag{1}$$

after fault d for the power injections $p \in \mathbb{R}^{|\Omega^B|}$ and lines Ω^L. Ω^B is the set of buses, and $|\Omega^B|$ and $|\Omega^L|$ are set-cardinalities, the number of buses and lines, respectively. $PTDF_d$ and the following approximations are only valid if and only if the system is still connected post-fault d, i.e., the system does not become islanded. The

$$PTDF_d \approx B_{br} \times A \times \tilde{B}^{-1}, \tag{2}$$

correspond to the lines in outage $\Omega_d^{\hat{L}} = \{l \,|\, y_l = 1,\, \forall l \in \Omega^L\}$, and has simultaneously $k = |\Omega_d^{\hat{L}}| = \sum_{l \in \Omega^L} y_l$ lines in outage. The binary variable y_l shows whether a line is in an outage, then $y_l = 1$, otherwise $y_l = 0$. B_{br}, A are the line reactance and incidence matrices defined in Appendix A and

$$\tilde{B}^{-1} \approx B^{-1} + \sum_{l \in \Omega^L} y_l F_l + \sum_{l \in \Omega^L} \sum_{\hat{l} \in \Omega^L} y_l y_{\hat{l}} G_{l,\hat{l}} + \sum_{l \in \Omega^L} \sum_{\hat{l} \in \Omega^L} \sum_{\check{l} \in \Omega^L} y_l y_{\hat{l}} y_{\check{l}} H_{l,\hat{l},\check{l}} \tag{3}$$

considers matrices F_l, $G_{l,\hat{l}}$ and $H_{l,\hat{l},\check{l}}$ of the lines in outage to get an altered inverse of the susceptance matrix B^{-1} that will be introduced later.

An objective is to obtain the y combinations that result in line overloads for k-simultaneous outages. The physical limits on the transmission lines are

$$-f_{\mathcal{L}}^B \le f_{\mathcal{L}} \le f_{\mathcal{L}}^B, \qquad \mathcal{L} \in \Omega^L \tag{4}$$

where $f_{\mathcal{L}}^B$ is the limit of the power flow over line $\mathcal{L}$. The conventional approach illustrated in Fig. 2(a) assesses many

contingencies d to determine the security of overloads. However, the conventional approach is impractical for many fault combinations k and many d.

The approach in this paper, illustrated in Fig. 2(b), formulates optimisations that provide the worst-case contingency, and then analysing the distribution of the QA solver provides the shortlist of contingencies. To identify the worst-case k-outage scenario that leads to overload on the line $\mathcal{L}$, the N-k security assessment can be formulated as a constrained mixed-integer nonlinear optimisation

$$\begin{aligned}
\underset{y,\lambda,f}{\text{maximize}} \quad & \lambda \\
\text{subject to} \quad & \lambda \le f_{\mathcal{L}}^{B} - f_{\mathcal{L}} \\
& \lambda \le f_{\mathcal{L}} - f_{\mathcal{L}}^{B} \\
& y_l y_{\hat{l}} \delta_{l,\hat{l}} \ge \delta^{B} \qquad \forall (l,\hat{l}) \in \Omega^{L} \\
& \sum_{l \in \Omega^{L}} y_l = k \\
& (1), (2), (3) \\
& y_l \in \{0,1\},
\end{aligned} \tag{5}$$

that maximises the constraint violation λ of (4). This approach may run the optimisation consecutively for the parameter $k = 1, 2, 3, \ldots$ until $\lambda \ge 0$. The constraint $y_l y_{\hat{l}} \delta_{l,\hat{l}} \ge \delta^B$ ensures that no outage combinations that have a shorter path than δ^B are considered, as the approximation from [24], Appendix A, is inaccurate for these. The constraints (1), (2), (3) are equality constraints (= replaces ≈). The approach returns

- value $k = \sum_{l \in \Omega^L} y_l$ as a metric for how many faults the system is secured against
- the values y_l as one combination of lines that triggers an N-k fault. Some solvers may also return multiple y_l combinations that have the same objective value.

A. Disjunctive PTDFs

The generic susceptance matrix

$$\begin{aligned}
\tilde{B}^{-1} \approx B^{-1} &+ \sum_{l \in \Omega^L} \sum_{\hat{l} \in \Omega^L} y_l y_{\hat{l}} B^{-1} I V_l B^{-1} - \sum_{l \in \Omega^L} y_l B^{-1} I V_l B^{-1} \\
&+ \sum_{l \in \Omega^L} \sum_{\hat{l} \in \Omega^L} \sum_{\check{l} \in \Omega^L} y_l y_{\hat{l}} y_{\check{l}} B^{-1} U_{\hat{l}} I V_l B^{-1} \\
&- \sum_{l \in \Omega^L} \sum_{\hat{l} \in \Omega^L} y_l y_{\hat{l}} B^{-1} U_{\hat{l}} I V_l B^{-1} \\
&- \sum_{l \in \Omega^L} \sum_{\hat{l} \in \Omega^L} y_l y_{\hat{l}} B^{-1} I E_l^{-1} V_{\hat{l}} B^{-1} \\
&- \sum_{l \in \Omega^L} \sum_{\hat{l} \in \Omega^L} \sum_{\check{l} \in \Omega^L} y_l y_{\hat{l}} y_{\check{l}} B^{-1} U_{\check{l}} E_l^{-1} V_{\hat{l}} B^{-1},
\end{aligned} \tag{6}$$

considers the combination of line outages of the lines Ω^L. [24] derived $\tilde{B}^{-1}$, summarized in Appendix A. Grouping the terms

$$\begin{aligned}
F_l &:= -B^{-1} I V_l B^{-1} \\
G_{l,\hat{l}} &:= B^{-1} I V_l B^{-1} - B^{-1} U_{\hat{l}} I V_l B^{-1} - B^{-1} I E_l^{-1} V_{\hat{l}} B^{-1} \\
H_{l,\hat{l},\check{l}} &:= B^{-1} U_{\hat{l}} I V_l B^{-1} - B^{-1} U_{\check{l}} E_l^{-1} V_{\hat{l}} B^{-1}
\end{aligned} \tag{7}$$

provides the compact formulation in (3). However, note this approximation is inaccurate for physically close faults [24] and not defined for faults that lead to islanded systems. The distance $\delta_{l,\hat{l}}$ between the two lines $(l,\hat{l})$ provides a metric for proximity. The combinations of two-lines

$$\Omega^{FL} = \left\{ (l,\hat{l}) | \{ l \ne \hat{l}, \delta_{l,\hat{l}} \ge \delta^B, (l,\hat{l}) \in \Omega^L \} \right\} \tag{8}$$

sufficiently far away when the distance is above the threshold δ^B. Two-line combinations too close to each other are

$$\Omega^{CL} = \left\{ (l,\hat{l}) | \{ l \ne \hat{l}, \delta_{l,\hat{l}} < \delta^B, (l,\hat{l}) \in \Omega^L \} \right\}. \tag{9}$$

This ensures the considered faults are sufficiently far away; however, it does not guarantee the fault combinations do not lead to islanded systems.

B. Quadratic Reformulation of Line Flow Limits

As QA can only consider quadratic unconstrained binary optimisations, we reformulate the cubic (3) to a quadratic boolean equation using auxiliary variables [42]. The bijective function

$$h : \Omega^C \to \Omega^{FL} \tag{10}$$

assigns a unique $c \in \Omega^C$ to each combination of the lines sufficiently far away $(l,\hat{l}) \in \Omega^{FL}$ from (8), where $\Omega^C = \{1, 2, \ldots |\Omega^{FL}|\}$, hence $(l,\hat{l}) = h(c)$. Subsequently, we introduce the binary auxiliary variable

$$z_c = y_l y_{\hat{l}}, \qquad \forall c \in \Omega^C, \tag{11}$$

indicating that two lines $(\hat{l}, l)$ are simultaneously in an outage, then $z_c = 1$, otherwise $z_c = 0$. We then define

$$\begin{aligned}
\mathcal{F}_l &:= F_l + G_{l,l} + H_{l,l,l} \qquad \forall l \in \Omega^L \\
\mathcal{G}_c &:= \frac{1}{2}(G_{l,\hat{l}} + G_{\hat{l},l}) \qquad (l,\hat{l}) = h(c),\ \forall c \in \Omega^C \\
\mathcal{H}_{l,c} &:= \frac{1}{2}(H_{l,\hat{l},\check{l}} + H_{l,\check{l},\hat{l}}) \qquad (\check{l},\hat{l}) = h(c),\ \forall l \in \Omega^L,\ c \in \Omega^C
\end{aligned} \tag{12}$$

where $\mathcal{G}_c$ and $\mathcal{H}_{l,c}$ are the averages of the symmetric assignments, e.g. $l, \hat{l}$ and $\hat{l}, l$. We then write compactly (3) as

$$\begin{aligned}
\tilde{B}^{-1} \approx B^{-1} &+ \sum_{l \in \Omega^L} y_l \mathcal{F}_l + \sum_{c \in \Omega^C} z_c \mathcal{G}_c \\
&+ \sum_{l \in \Omega^L} \sum_{c \in \Omega^C} y_l z_c \mathcal{H}_{l,c}.
\end{aligned} \tag{13}$$

The two inequality constraints for physical limits (4) on the transmission lines are then

$$\begin{aligned}
-f^B \le B_{br} A B^{-1} p &+ \sum_{l \in \Omega^L} y_l B_{br} A \mathcal{F}_l p + \sum_{c \in \Omega^C} z_c B_{br} A \mathcal{G}_c p \\
&+ \sum_{l \in \Omega^L} \sum_{c \in \Omega^C} y_l z_c B_{br} A \mathcal{H}_{l,c} p \le f^B,
\end{aligned} \tag{14}$$

Algorithm 1: Search for N-k Security With QUBOs.

Input: k_0, $\mathcal{P}^A$, $\mathcal{P}^B$, $\mathcal{P}^C$, $\mathcal{P}^D$, f^B, δ, δ^B
Output: $k, y, \mathcal{L}$
$u \leftarrow 0, k \leftarrow k_0$, $\lambda^+_{\mathcal{L}} = 0, \lambda^-_{\mathcal{L}} = 0$ **while** $(\lambda^+_{\mathcal{L}} \leq 0) \wedge (\lambda^-_{\mathcal{L}} \leq 0)$ **do**
  $\mathcal{L} \leftarrow o(u)$
  Solve (16) with $\lambda^+_{\mathcal{L}}$ and $\lambda^-_{\mathcal{L}}$, respectively
  if $u = |\Omega^L|$ **then**
    $k \leftarrow k + 1$
    $u \leftarrow 0$
  else
    $u \leftarrow u + 1$

where $f^B \in \mathbb{R}^{+|\Omega^L|}$ are the line power limits. We define for all lines $\mathcal{L} \in \Omega^L$ the post-fault overloading

$$\lambda^{\pm}_{\mathcal{L}} = \mp f^B_{\mathcal{L}} \pm \mathcal{P}^A_{\mathcal{L}} \pm \sum_{l \in \Omega^L} y_l \mathcal{P}^B_{l,\mathcal{L}} \pm \sum_{c \in \Omega^C} z_c \mathcal{P}^C_{c,\mathcal{L}} \pm \sum_{l \in \Omega^L} \sum_{c \in \Omega^C} y_l z_c \mathcal{P}^D_{l,c,\mathcal{L}} \quad \forall \mathcal{L} \in \Omega^L \tag{15}$$

where $\mathcal{P}^A_{\mathcal{L}} := B_{br} A B^{-1} p$, $\mathcal{P}^B_{l,\mathcal{L}} := B_{br} A \mathcal{F}_l p$, $\mathcal{P}^C_{c,\mathcal{L}} := B_{br} A \mathcal{G}_c p$ and $\mathcal{P}^D_{l,c,\mathcal{L}} := B_{br} A \mathcal{H}_{l,c} p$. $\lambda^{\pm}_{\mathcal{L}} \leq 0$ is equivalent to the physical limit (14). These reformulations modify the optimisation (5) to a Mixed Integer Program with Quadratic terms in the Constraints (MIQCP) that can be solved with commercial, conventional solvers.

III. Quantum Annealing Based Approach

A. Search With Many Quadratic Unconstrained Optimisations

The approach consecutively searches over k solving for each line $\mathcal{L}$ the two QUBOs

$$\begin{aligned} \underset{y,z}{\text{maximize}} \quad & \lambda^{\pm}_{\mathcal{L}} - C_1 \left(k - \sum_{l \in \Omega^L} y_l \right)^2 \\ & - C_2 \left(\sum_{c \in \Omega^C,\, (l,\hat{l}) = h(c)} y_l y_{\hat{l}} - 2 y_l z_c - 2 y_{\hat{l}} z_c + 3 z_c \right) \\ & - C_3 \sum_{(l,\hat{l}) \in \Omega^{CL}} y_l y_{\hat{l}}, \end{aligned} \tag{16}$$

where $y \in \{0,1\}^{|\Omega^L|}$, $z \in \{0,1\}^{|\Omega^C|}$. The optimisation exclusively considers binary variables and maximises the physical constraint violations $\lambda^{\pm}_{\mathcal{L}}$ defined in (15) for the lower and upper bounds ($\pm$ corresponds to the two optimisations). The parameters are the simultaneous line faults k considered, the flow parameters $\mathcal{P}^A_{\mathcal{L}}$, $\mathcal{P}^B_{l,\mathcal{L}}$, $\mathcal{P}^C_{c,\mathcal{L}}$, $\mathcal{P}^D_{l,c,\mathcal{L}}$, $f^B_{\mathcal{L}}$, the distances between two lines $\delta_{l,\hat{l}}$ and the threshold δ^B to ensure an accurate approximation of the PTDFs [24]. C_1 penalises deviations from $\sum_{l \in \Omega^L} y_l = k$. C_2 penalises deviations from (11), and C_3 penalises two line faults too close (9) that would lead to invalid PTDF approximations, i.e. $\mathcal{P}^A_{\mathcal{L}}$, $\mathcal{P}^B_{l,\mathcal{L}}$, $\mathcal{P}^C_{c,\mathcal{L}}$, $\mathcal{P}^D_{l,c,\mathcal{L}}$ would not be accurate. This optimisation can assess the security of the line $\mathcal{L}$ for all k-faults that are sufficiently far apart, e.g. if $\lambda^+_{\mathcal{L}} \leq 0$,and $\lambda^-_{\mathcal{L}} \leq 0$, then the line $\mathcal{L}$ is not overloaded for any k-fault combination.

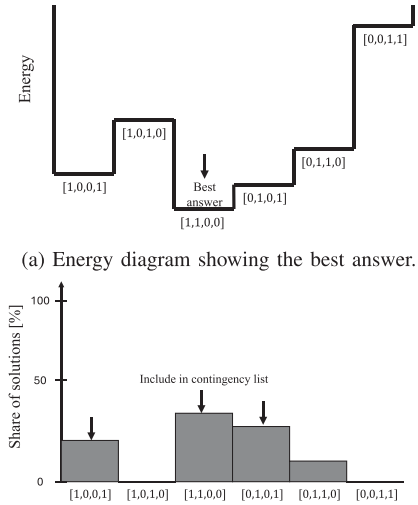

(a) Energy diagram showing the best answer.

(b) Distribution of solutions using QA showing low-energy solutions.

Fig. 3. Using QA to identify contingency list: in (a) the energy diagram over the 4 binary variables in one of the QUBOs assessing $k = 2$ and in (b) the distribution of solutions from running QA multiple times. Typically (b) is used to identify the best solutions; however, this approach uses the distribution to collect the list of contingencies as each low-energy solution corresponds to a $k = 2$ contingency scenario.

The search approach starts after computing the pre-fault flows $f^0 = B_{br} \times A \times B^{-1} \times p$. Subsequently, the approach orders the lines $\mathcal{L}$ according to their pre-fault loading levels $|f^0_{\mathcal{L}}|$. The function

$$o : \{0, 1, 2 \ldots u, \ldots |\Omega^L|\} \rightarrow \Omega^L \tag{17}$$

outputs the line $\mathcal{L}$ with the uth largest $|f^0_{\mathcal{L}}|$, e.g. so that $|f^0_{\mathcal{L}1}| \leq |f^0_{\mathcal{L}2}|$, where $\mathcal{L}1 = o(u)$ and $\mathcal{L}2 = o(u+1)$, respectively. The Algorithm 1 iterates u solving the QUBOs (16) for each line $\mathcal{L}$ and for increasing k simultaneous faults until the first overload has been found. The solution to the last optimisation y provides one combination of faults resulting in an overload at line $\mathcal{L}$. Note that the embeddings mapping the QUBO problem to the quantum computing hardware are derived only once, and the spin biases are just updated for each line $\mathcal{L}$ and for k.

B. Contingency List From Distribution of Annealing Outputs

QA approaches the QUBO problems to optimality by a process called 'annealing'. The probability of a qubit being assigned as 0 or 1 is controlled by a qubit bias and coupling qubits together. Ultimately, the QUBO (16) problem can be written as $\underset{y,z}{\text{maximize}} [y, z]^T \mathcal{Q} [y, z]$ with the real-valued upper triangular matrix $\mathcal{Q}$. The diagonal of $\mathcal{Q}$ shows the qubit biases, and the couplings are the off-diagonal elements in this matrix. Fig. 3(a) illustrates the relative energy of 6 different states of the 4 variables $[y, z]$ that depend on the bias and couplings. The dimensions of $\mathcal{Q}$ is not directly dependent on the power network

system size ($|\Omega^B|, |\Omega^L|$), however, on the number of lines in the contingency list (y may relate only to a subset $\subset |\Omega^L|$) and the two-line combinations (z) thereof.

QA starts from a quantum-mechanical superposition of all states, where qubit states are possibly entangled. During annealing, the states change according to the energy landscape from the applied bias and couplings, eventually leading to a state with the lowest energy (best answer as Fig. 3(a) shows). QA is a stochastic process, meaning different runs can lead to different local minima with low energy, but possibly not the lowest. Therefore, Fig. 3(b) shows that distributions of solutions can be obtained by running annealing multiple times on the same problem.

Our approach uses the distribution to obtain the N-k contingency shortlist Ω^Y. The optimisation (16) represents the security assessment. Typically, optimisations provide just a single solution, here worst-case contingency. However, by QA that leverages quantum effects, we can assess all possible contingencies. The distribution provides a shortlist of contingencies. We consider $\hat{\Omega}^Y$ the set of solutions where each $d \in \hat{\Omega}^Y$ corresponds to a different $[y,z]_d$ solution with objective value $\lambda_{\mathcal{L},d}$. The following holds $[y,z]_{d1} \neq [y,z]_{d2}$, $\forall d1, d2 \in \hat{\Omega}^Y$, $d1 \neq d2$; and $y_l = 1, \forall l \in \Omega^{\hat{L}}_d$; and $y_l = 0, \forall l \in \Omega^L \setminus \Omega^{\hat{L}}_d$. ρ_d is the share of runs that produced solution d where $\sum_{d\in\hat{\Omega}^Y} \rho_d = 1$. The conventional approach is to take the best answer d^* or $[y,z]^*$ (worst-case contingency) where $\lambda_{\mathcal{L},d^*} = \max\{\lambda_{\mathcal{L},d}, d \in \hat{\Omega}^Y\}$ among all solutions from the various annealing runs, e.g. Fig. 3(a). However, as Fig. 3(b) shows, we apply the cutoff threshold $\bar{\rho}$ to obtain the contingency shortlist $\Omega^Y = \{d \,|\, \rho_d \geq \bar{\rho}, \forall d \in \hat{\Omega}^Y\}$. Subsequently, for a more accurate estimation of the overloads, we compute the line flows $f_{\mathcal{L}}$ using the actual $PTDF_d$ from (28) in (1), then, evaluating the overloads $\overline{\lambda}_{\mathcal{L},d} = \max\{0, f^B_{\mathcal{L}} - f_{\mathcal{L}}, f_{\mathcal{L}} - f^B_{\mathcal{L}}\} \forall d \in \Omega^Y$. Finally, we obtain the worst-case contingency d^* by evaluating the overloads computed with actual PTDFs, e.g. $\overline{\lambda}_{\mathcal{L},d^*} = \max\{\overline{\lambda}_{\mathcal{L},d}, d \in \hat{\Omega}^Y\}$.

C. Errors by Quantum Annealer and Neumann Series

Two errors are superimposed when obtaining the contingency lists from the QA. The annealer itself is a heuristic making (quantum) errors, and the Neumann series approximates the PTDFs, introducing errors. The average absolute error of the approximation of the Neumann series is $\sum_{d\in\Omega^Y} \frac{1}{|\Omega^Y|} |\overline{\lambda}_{\mathcal{L},d} - \lambda_{\mathcal{L},d}|$. As a baseline, computing the ground truth of identifying the worst-case contingencies requires to evaluate all of the N-k faults Ω^D also using the actual $PTDF_d$ from (28) in (1), e.g. $\lambda_{\mathcal{L},d} = \max\{0, f^B_{\mathcal{L}} - f_{\mathcal{L}}, f_{\mathcal{L}} - f^B_{\mathcal{L}}\} \forall d \in \Omega^D$. Then, identify $\lambda_{LODF} = \max\{\lambda_{\mathcal{L},d}, \forall d \in \Omega^D\}$. The residual error of this approach is $|\lambda_{\mathcal{L},d^*} - \lambda_{LODF}|$.

D. Meta-Heuristic For a Finite Number of Qubits

Quantum computers have a limited number of qubits Q and fixed couplings between these qubits. As the derived QUBO problem involves linear and quadratic terms that describe the coupling between variables, the problem variables and couplings need to be embedded (matched) to the fixed coupling of the quantum computer hardware, e.g. matching one graph to another graph. For large power grids, the number of binary variables is large and likely no fitting embedding can be found directly. Hybrid solvers address this issue, firstly finding a suitable embedding and breaking the problem into sub-problems solved with the quantum computing unit. The number of binary variables required for the above problem is $|\Omega^L| + |\Omega^C|$, and $Q \leq |\Omega^L| + |\Omega^C|$ for large power systems.

We propose dividing the problem into smaller sub-problems and, for each, derive an embedding. Each subproblem i includes all binary variables y_l with $l \in \Omega^L$ and a subset $\Omega^C_i \subseteq \Omega^C$ of binary variables of two-line combinations $z_c \in \Omega^C_i$. Therefore, replacing (11) by

$$z_c = y_l y_{\hat{l}}, \qquad \forall c \in \Omega^C_i, \tag{18}$$

and adding

$$y_l + y_{\hat{l}} \leq 1, \qquad (l,\hat{l}) = h(c), \forall c \in \{\Omega^C - \Omega^C_i\}. \tag{19}$$

Making these modifications in QUBO (16) requires changing the second penalty term to

$$-C_2 \left(\sum_{c\in\Omega^C_i,\,(l,\hat{l})=h(c)} y_l y_{\hat{l}} - 2y_l z_c - 2y_{\hat{l}} z_c + 3z_c \right) \tag{20}$$

and adding to the third penalty term

$$-C_3 \left(\sum_{(l,\hat{l})\in\Omega^{CL}} y_l y_{\hat{l}} + \sum_{\substack{c\in\{\Omega^C-\Omega^C_i\},\\ (l,\hat{l})=h(c)}} y_l y_{\hat{l}} \right) \tag{21}$$

to penalise the two-line fault combinations $\{\Omega^C - \Omega^C_i\}$. The size of the subset $|\Omega^C_i| \leq Q - |\Omega^L|$ is limited by the available qubits Q, the possible embeddings and connectivity of qubits.

This paper applies a Monte-Carlo-type sampling approach to cover most N-k contingencies. There, the sub-problem subsets Ω^C_i are uniformly randomly drawn without replacements, so $\Omega^C_i \subset \Omega^C$, $\forall i = 1, 2, 3, \ldots I$. The probability of a fault $\Omega^{\hat{L}}$, with $|\Omega^{\hat{L}}| \leq k$, being represented by the two-line combinations Ω^C_i is

$$\mathbb{P}\left(\Omega^{\hat{L}} \subset \{f(c) : \forall c \in \Omega^C_i\}\right) \geq \left(\frac{|\Omega^C_i|}{|\Omega^C|}\right)^{R(\frac{k}{2})}, \tag{22}$$

where $R : \mathbb{R} \to \mathbb{Z}$ rounds down to the closest integer that is smaller. If the connectivity of the qubits is sufficient, we recommend selecting $|\Omega^C_i|$ as high as possible, e.g. $|\Omega^C_i| = Q - |\Omega^L|$, to reduce the number of runs by the quantum annealer if the quantum hardware allows for full qubit connectivity. We recommend drawing

$$I = \left(\frac{|\Omega^C_i|}{|\Omega^C|}\right)^{-R(\frac{k}{2})} \tag{23}$$

uniformly random subsets with Monte-Carlo sampling to robustly assess the N-k security, aiming to cover with high probability most k faults. The modified Algorithm 2 is nested and requires significantly longer to execute. There, we follow (23),

Algorithm 2: Meta-Heuristic for N-k Security With Limited Qubits.

Input: k_0, $\mathcal{P}^A$, $\mathcal{P}^B$, $\mathcal{P}^C$, $\mathcal{P}^D$, f^B, δ, δ^B, I, drawn $\Omega_i^C \subset \Omega^C, \forall i = 1, 2, \dots I$

Output: $k, y, \mathcal{L}$

$u \leftarrow 0, k \leftarrow k_0$, $\lambda_{\mathcal{L}}^+ = 0, \lambda_{\mathcal{L}}^- = 0$ **while** $(\lambda_{\mathcal{L}}^+ \leq 0) \wedge (\lambda_{\mathcal{L}}^- \leq 0)$ **do**

- $\mathcal{L} \leftarrow o(u)$
- $i \leftarrow 0$
- **while** $i \leq I$ **do**
  - Solve (16) modified by (20), (21) for Ω_i^C
  - $i \leftarrow i + 1$
- **if** $u = |\Omega^L|$ **then**
  - $k \leftarrow k + 1$
  - Compute I with (23)
  - Randomly draw $\Omega_i^C \subset \Omega^C, \forall i = 1, 2, \dots I$,
  - $u \leftarrow 0$
- **else**
  - $u \leftarrow u + 1$

more random subsets Ω_i^C need to be drawn with increasing k to cover all k-faults with high probability.

This proposed Algorithm 2 has some interesting scaling properties. Creating I embeddings is typically a computationally expensive step; however, this algorithm requires creating embeddings only once. The same embeddings I can be used for all lines $\mathcal{L} \in \Omega^L$ and for other operating conditions that each update $\mathcal{P}^A$, $\mathcal{P}^B$, $\mathcal{P}^C$ and $\mathcal{P}^D$. Furthermore, the same embeddings can be used for all k as only the k parameter is updated in the optimisation (16).

IV. Case Study

The IEEE 118-bus system was primarily used to test the proposed approach. The 300-bus system, 1354 pegase system, and 2383 wp system were used from MATPOWER, in a brief scaling analysis. In the IEEE 118-bus system, to study the PTDFs, 70 faults were randomly sampled that do not lead to islanded systems, 10 each for $k = \{1, 2 \dots 7\}$. These fault combinations had a minimum shortest distance of $\delta > \delta^B = 2$ between the lines in an outage. The operating load levels were sampled from a Kumaraswamy distribution (1.6, 2.8) around $\pm 25\%$ of the nominal loads, having a Pearson correlation coefficient 0.75. The generator levels were assigned with a DC OPF. The security assessment considered that the line loading limits were set at 230 MW for all lines. A security label was computed per line (e.g. overloaded then insecure, if not overloaded, then secure). The Dijkstra algorithm was considered to compute the distances δ between the lines. Python was used on a standard laptop with an Intel i7 core. The QA and DWaves Hybrid CQM solver was used to map the problem to the quantum hardware and determine the penalisation scalar values C_1, C_2 and C_3. GUROBI and exhaustive search were used as baselines. All solvers had default settings.

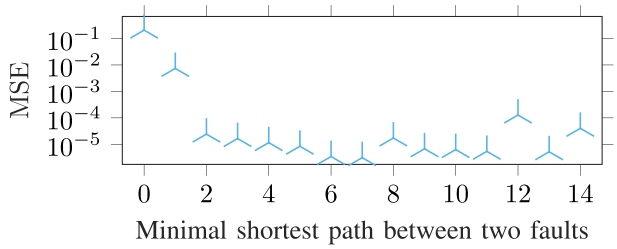

Fig. 4. Element-wise MSE of approximating the actual $(B + UIV)^{-1}$ with $\tilde{B}^{-1}$ for $k = 2$ faults with different minimal distances δ. The approximation seems sufficiently accurate for $\delta \geq \delta^B$ where $\delta^B = 2$.

TABLE I
Share of Line Combinations $(l, \hat{l})$ With Shortest Distance δ in [%] and Share of Far Combinations $\frac{|\Omega^{FL}|}{|\Omega^L||\Omega^L|}$ With Threshold δ^B.

δ	0	1	2	3	4	5	6	7	8	9	10	11	12	13
Share	3.4	7	10.2	11.9	12.7	13.1	12	10.4	7.9	5.1	3.4	2	0.8	0.1
$\frac{\lvert\Omega^{FL}\rvert}{\lvert\Omega^L\rvert\lvert\Omega^L\rvert}$	100	96.6	89.6	79.4	67.5	54.8	41.7	29.7	19.3	11.4	6.3	2.9	0.9	0.1

TABLE II
Security Assessment With Power Transfer Distribution Factors With Mean and Standard Deviation in Brackets.

k	1	2	3	4	5	6	7
$\Delta\lvert f_{\mathcal{L}}\rvert$ / $\lvert f_{\mathcal{L}}\rvert$ [%]	0(0)	6(9)	23(10)	31(20)	50(17)	88(33)	109(54)
Accuracy [%]	100	100	99	99	98	96	95
False [%]	0	0	0	1	1	2	3
Missed [%]	0	0	1	0	1	2	2

A. Approximate Disjunctive Power Transfer Distribution Factors

This study investigates the approximation error of the disjunctive PTDFs from Appendix A, selecting δ^B, and the impact on security assessment. Studying this adds perspective to the QA error studied later. The Neumann series approximation may be inaccurate depending on the proximity of the faults. There, the MSE was assessed between the two $(B + UIV)^{-1}$ and $\tilde{B}^{-1}$ for 10000 different $k = 2$ fault combinations. Fig. 4 shows the MSE plateaus after distance $\delta^B \geq 2$, motivating that selection. Table I shows the share of two-line combinations $\frac{|\Omega^{FL}|}{|\Omega^L||\Omega^L|}$ that are considered far apart when selecting the value of δ^B (e.g. when $\delta^B = 2$ this share was at 89.6% totalling at $|\Omega^{FL}| = 15581$). However, selecting $\delta^B \geq 2$ means faults closer than a distance of 2 are not considered in this security assessment. In the 118-bus system, this share was around 90% of $k = 2$ faults that can still be considered; however, with increasing k, this share decreased.

Table II shows the impact of the approximation on the security for faults with $\delta^B \geq 2$. 91% were secure conditions. The relative difference in line flow estimations stays below 50% for $k < 4$; however, the difference increases for higher k. Still, the accuracy is above 95% accuracy for $k \leq 5$, however, the accuracy decreases below 90% for higher k values. The false and missed alarms increased similarly with k. The approach is only accurate for $k \leq 4$ in the IEEE 118-bus system.

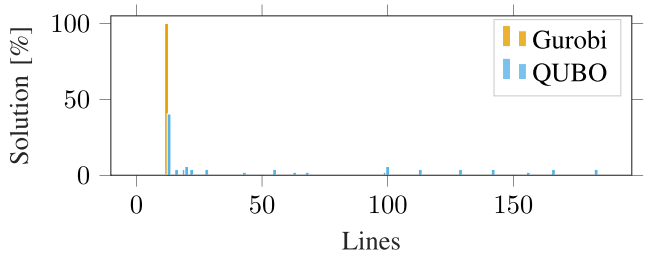

Fig. 5. Identifying the worst-case $k = 1$ fault on an arbitrary selected line $\mathcal{L} = 0$. The fault on line $l = 12$ causes the highest overload on $\mathcal{L} = 0$.

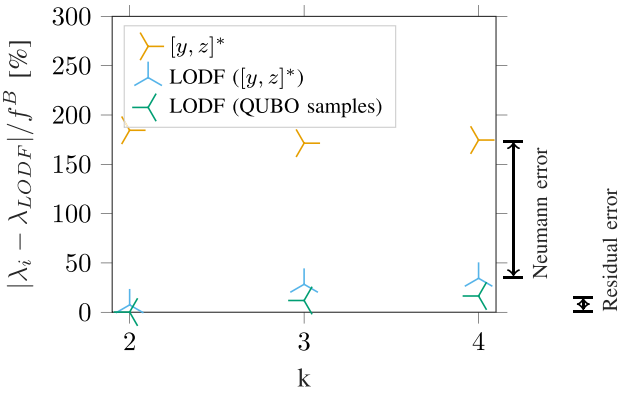

Fig. 6. The approach minimises inaccuracies: the approximation error from the Neumann series is superposed by the optimality gap from the annealing process leading to suboptimal worst-case contingency ($[y, z]^*$). However, the proposed approach analyses all local optima from annealing (QUBO samples) to more optimally identify contingencies that are within a residual $< 15\%$ range to the worst-case contingency in $k = 4$. The reference λ_{LODF} is the ground truth of worst-case line loading.

B. N-k Security Assessment by Mitigating Quantum Errors

This case study investigates whether the quantum program can accurately assess security. As Fig. 5 shows, the annealer does not always solve the optimisation to (global) optimality, as the QUBOs and GUROBI outputs sometimes differ. Two errors occur: one error is caused by the annealer, and the other error is caused by the Neumann series approximating the PTDFs. These errors lead to inaccuracies that superpose and may lead to inaccurate security estimations, e.g. that an overload is identified as worst-case, which is not the worst-case contingency. Testing these errors, we use the MIQCP reformulation Section II and the exhaustive LODF-search as baselines (reference λ_{LODF}). We compute the relative error to this reference, identifying the worst-case contingency as in Section III-C. We report average errors for 10 loading conditions, randomly selected $|\Omega^L| = 50$ and random $\mathcal{L}$ lines. 60 QUBOs were solved ($\lambda^+_{\mathcal{L}}$ and $\lambda^-_{\mathcal{L}}$ in Algorithm 1).

Fig. 6 shows that QA produces a set of low-energy samples where the sample with the highest objective value ($[y, z]^*$) is not necessarily the contingency leading to the highest line overload. However, the worst-case contingency is among the samples with an overload error of less than 5%, 10%, 15% close to the actual contingency with the highest overload (reference λ_{LODF}) for $k = 2, 3, 4$, respectively. These results confirm that QA can identify multiple high-impact contingencies at the same time from the QUBO samples. Table III shows that the worst-case contingencies are within the obtained distribution at all $k = 2$ cases. While for $k > 2$ the specific global solution is not part of the QA distribution, often the solutions overlap in individual lines and the residual error of the QA solutions is shown in Fig. 6 within an error of $< 15\%$. This misidentification is due to the two superposing errors of the annealer and the PTDF approximation studied in this and the previous case study. Specifically, the inaccuracy in the PTDFs increases with k as Section IV-A studied, and is here too large to accurately identify the $k > 2$ worst-case contingency. Nonetheless, the proposed approach identifies a set of critical k-contingencies that have similarly large line loading as the worst-case contingency (Fig. 6).

TABLE III
COMPARING WORST-CASE k LINE FAULT COMBINATION (CORRECT FROM EXHAUSTIVE SEARCH), AND OBTAINED FROM QA.

$\mathcal{L}$	k	Correct	QA worst-case	Correct in QA distribution
4	2	[32 50]	[32 140]	X
4	3	[8 63 160]	[37 115 140]	
4	4	[8 112 174 169]	[23 37 115 140]	
142	2	[122 142]	[106 128]	X
142	3	[42 122 142]	[106 128 137]	
142	4	[27 42 122 142]	[37 106 128 137]	
143	2	[160 131]	[129 160]	X
143	3	[131 155 160]	[129 140 169]	
143	4	[131 155 160 175]	[115 140 148 169]	
149	2	[128 150]	[128 137]	X
149	3	[115 128 150]	[128 137 150]	
149	4	[39 115 128 150]	[128 137 150 169]	
15	2	[19 36]	[36 106]	X
15	3	[19 23 36]	[6 20 106]	
15	4	[6 44 108 154]	[6 20 49 106]	
40	2	[37 40]	[37 40]	X
40	3	[24 37 40]	[37 40 140]	
40	4	[24 37 40 176]	[37 40 140 176]	
80	2	[47 75]	[82 83]	X
80	3	[53 75 184]	[82 83 133]	
80	4	[53 75 109 133]	[82 83 128 133]	

C. Obtaining Contingency Lists With QA

This study investigates whether the output of the annealer (with $Q = 1500$) can be used for impact analysis of the grid, leading to a contingency list and tests Section III-B. As illustrated in Fig. 3, the annealer provides samples that have the lowest 'energy' (objective value), where often the sample with the lowest 'energy' corresponds with the optimal decisions, e.g. see the comparison in Fig. 5. Fig. 5 shows that the global optimal solution from GUROBI matches the most frequent solution obtained by the annealer. If a cutoff value $\bar{\rho} = 25\%$ is applied, only the line 12 is shortlisted $\Omega^Y = \{12\}$, which matches with the worst-case contingency found by GUROBI. However, the proposed approach can lower the threshold to $\bar{\rho} = 5\%$, and a more conservative contingency shortlist $\Omega^Y = \{12, 19, 99\}$ is obtained. These additional lines $l = 19$ and $l = 99$, also have a high impact on the system under k contingencies. This demonstrates that multiple low-energy solutions can be obtained with the QA. Low-energy solutions correspond to high-impact

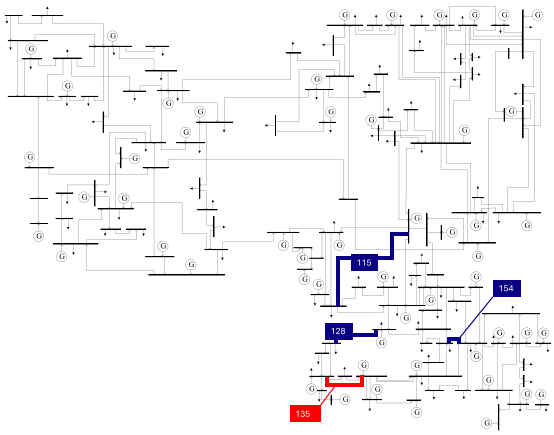

Fig. 7. IEEE 118-bus system showing worst-case $k = 3$ combination (blue marked lines) for overloading line $\mathcal{L} = 135$ (red). This output is from one iteration in Algorithm 1.

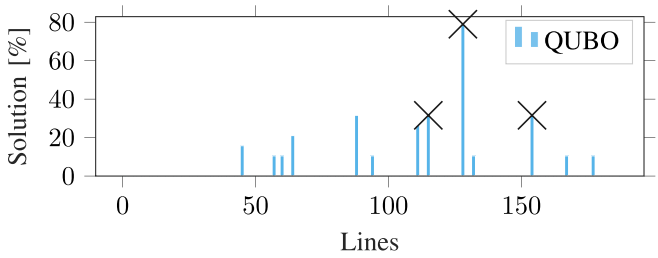

Fig. 8. Assessing the impact of using quantum annealers' output distribution of solutions for the selected line $\mathcal{L} = 135$. The worst $k = 3$ combination is marked with X. GUROBI can not compute for $k = 3$.

contingencies on the system. Nonetheless, such a list can also be obtained using the LODFs for all lines and ranking the overloads, which may take more time than the quantum program, as we will investigate in Section IV-E.

D. Line Reinforcements Leveraging Quantum Effects

This use case investigates the distribution of the output of quantum annealers to identify lines as candidates for reinforcements, e.g., lines that are particularly likely to result in network overload when failing. Faults 115, 154 and 128 are the worst-case $k = 3$ combination for overloading line 135 as illustrated in Fig. 7. However, Fig. 8 shows that line 128 is present multiple times in many $k = 3$ combinations, not only in the worst-case, suggesting reinforcing line 128 can improve robustness against many $k = 3$ fault combinations. Executing the full Algorithm 1 leads to the full distribution from where the weakest link that reduces overloads on $\mathcal{L}$ can be identified. For $k = 4$ and 6 overloaded lines, Fig. 9(a) shows such a full distribution, where the four top (weakest) lines that may be reinforced are 37,128,140 and 137 as shown in Fig. 9(b). The lines to reinforce are in the same area where the overloads are to be minimised (red lines). Reinforcing these lines may then reduce the overloads on the red lines at multiple outages.

E. Computational Times

This case study investigates the computational performance and estimates the scaling to the full system. This study

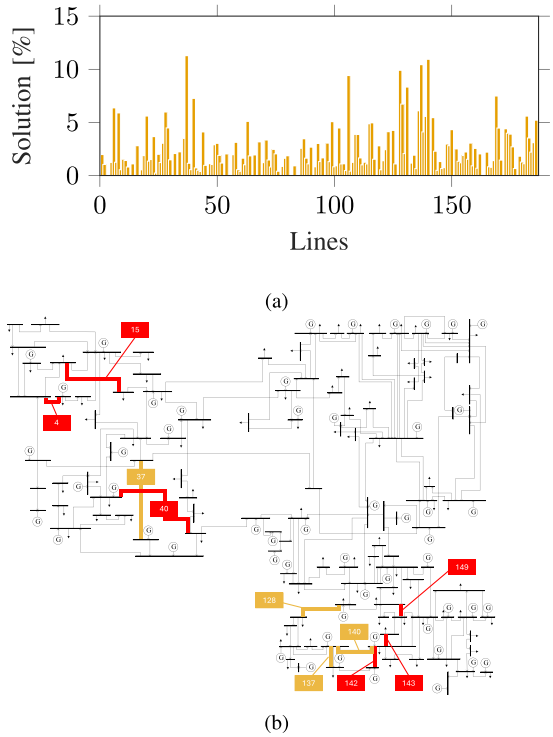

Fig. 9. Analysing QA distribution (a) across 6 overloaded lines (red in b) from all $k = 4$ simultaneous failures in 50 lines shows some lines are more present in the worst-case faults than others. For example, the top four lines in yellow shown in (b) can be reinforced to improve network resilience for $k = 4$ faults.

TABLE IV
GUROBI MIQCP SOLVER TIMES (SECOND) ARE AVERAGES OF 10 RUNS WITH STANDARD DEVIATION IN BRACKET. 187 LINE FAILURES WERE CONSIDERED FOR ONE POSSIBLY OVERLOADED LINE $\mathcal{L}$.

k	Time	binary variables	constraints
1	1092(43)	15768	17394
2	1291(153)	15768	17394

considers two baselines, GUROBI solving the MIQCP introduced in Section II and an exhaustive search assessing all contingencies with LODFs, representing a state-of-the-art forward screening of contingencies. As a baseline, Table IV shows the computation time, number of binary variables and constraints when GUROBI assesses all k -faults for the security of a single line (as illustrated in Fig. 7 assessing all blue combinations that could overload a single line). These computation times of this baseline are similar to a MINLP formulation from [2], showing 900s to identify the worst-case $k = 2$ contingency in the IEEE 118-bus system versus 1291s as in this work.

Studying our approach, we investigate the computational performance on 10 random iterations from Algorithm 1, 10 different operating loading conditions, and 10 randomly selected lines to check for overloads, considering $|\Omega^L| = 50$ randomly selected line outages, considering all k combinations. Overall 60 QUBOs were solved (λ^+ and Λ^- optimisations for $k = 2, 3, 4$). These QUBOS had in average 1144 binary variables with a standard deviation of 12. Table V shows the proposed approach's CPU and QPU access time (total for λ^+ and Λ^- QUBOs). We also

TABLE V
COMPUTATIONAL TIMES (SECOND) OF TWO APPROACHES ASSESSING N-k SECURITY OF 50 LINE FAILURES ON ONE POSSIBLY OVERLOADED LINE $\mathcal{L}$. THE TABLE SHOWS AVERAGES OF 10 RUNS WITH STANDARD DEVIATION IN BRACKETS.

k	2	3	4
Exhaustive LODFs	18(4)	118(45)	1917(328)
QUBOs, CPU time	10.1(0.2)	10.1(0.1)	10.1(0.2)
QUBOs, QPU time	0.06(0.0001)	0.06(0.0001)	0.06(0.0001)

TABLE VI
MAX NUMBER OF LINES $|\Omega^L|$ THAT CAN BE CONSIDERED IN THE $k-$ CONTINGENCY LIST WHEN $Q = 1500$ AND THE NUMBER QUBOS REQUIRING SOLVING.

System	118-bus	300-bus	1354 pegase	2383 wp
max $\|\Omega^L\|$	57	56	55	55
Number of QUBOs (16)	374	822	3982	5792

TABLE VII
ESTIMATION OF COMPUTATIONS USING THE VARIOUS APPROACHES FOR THE FULL N-k SECURITY ASSESSMENT PROBLEM CONSIDERING 187 FAULTS AND ALL POSSIBLE 187 OVERLOADED LINES, EXCEPT THE DWAVE QUBO* APPROACH, IS N/A FOR 187 FAULTS AND HAS BEEN ASSESSED FOR 50 FAULTS INSTEAD AS THE QA IS LIMITED.

k		1	2	3	4
GUROBI MIQCP		57h	67h	N/A	N/A
Ex search LODFs		N/A	4min	3.5h	114h
DWave QUBOs*	QPU	N/A	N/A / 12s	N/A / 12s	N/A / 12s
	CPU	N/A	N/A / 31min	N/A / 31min	N/A / 31min

compare an exhaustive search using LODFs, showing that the proposed approach outperforms in scaling to more faults, as the CPU and QPU time is constant.

To estimate the computations of the baselines and illustrate the issue, we project (estimate) the computations for checking all 187 lines with LODFs (corresponding to $|\Omega^L| = 50$ lines) by multiplying with $\frac{k!(50-k)!}{50!}\frac{187!}{k!(187-k)!}$. Table VII shows GUROBI can not compute beyond $k > 2$, and exhaustive search requires 3.5h or 114h in $k = 3, 4$, respectively, which we expect is significantly worse in larger systems. We could not directly assess the computations of our QUBO approach as the DWAVE hardware is limited in the number of qubits; however, the table shows the comparison from the 50-lines case reported earlier.

Finally, we assess the impact of system size and the maximal number of lines that can be included in the contingency list, considering a limited annealer with $Q = 1500$. For four power systems, the study randomly assigns Ω^L with increasing $|\Omega^L|$ starting from $|\Omega^L| = 3, 4 \ldots$. The study then computes the combinations Ω^C, and finally assesses whether $Q \leq |\Omega^L| + |\Omega^C|$ is fulfilled. The study stops at the first $|\Omega^L|$ where the inequality is not met. This study did not consider the connectivity of the QA. As discussed in Section III-D, Table VI shows that the limit is the number of single lines as each line requires binary variables, and each combination requires binary variables ($Q \leq |\Omega^L| + |\Omega^C|$). Table VI shows that the system size does not impact the problem size on the quantum annealer; however, the system size impacts the number of QUBOs that need to be solved, i.e. each line in the transmission system requires solving two QUBOs (16). For

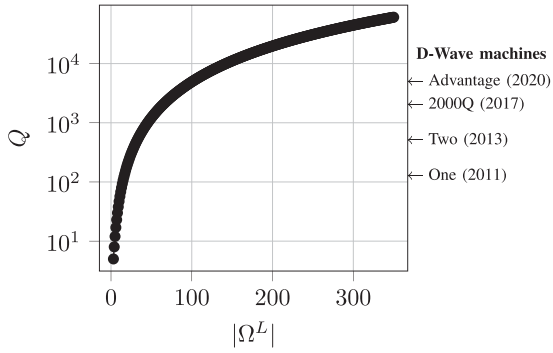

Fig. 10. The minimal qubits Q needed in the approach (16) to consider $|\Omega^L|$ lines and all k-combinations thereof in the Polish 2383wp system.

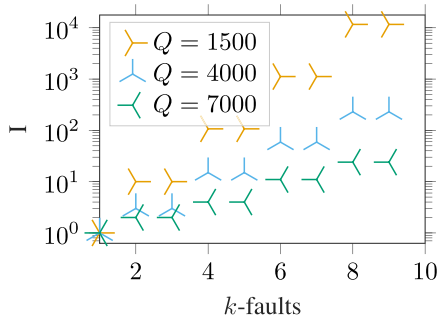

Fig. 11. The required samples I to perform the security assessment with a quantum computer of size Q.

the Polish system 2384 wp system, Fig. 10 shows the required qubits to consider $|\Omega^L|$ lines. This study demonstrates that current quantum annealers limit this application to an order of $|\Omega^L| \approx 50$.

F. Practical Approach for Annealers With Limited Qubits

This study investigates the meta-heuristic approach to various parameters that characterise the problem size (k, $|\Omega^L|$) and parameters characterising the approach (hardware with some qubits Q, the number of samples I). Algorithm 2 applies random subsets of two-line combinations $|\Omega^C|$ to keep the QUBOs solvable with Q qubits, e.g. a single QUBO i assesses one line loading for all k-fault combinations of the subset Ω^C_i. The number of two-line combinations $|\Omega^C|$ depends on the grid connectivity, the number of considered contingencies and the threshold δ^B, e.g. in the IEEE 118-bus system, the numbers $|\Omega^C| = 15581$ for $|\Omega^L| = 187$ lines. This initial study assumes all possible couplings on the annealer with qubits Q, the maximal $|\Omega^L| + |\Omega^C| = Q$. Then, Fig. 11 shows the required number of samples I (see (23)) where the approach can identify the worst-case contingency. Fig. 12 shows the probability of identifying the worst-case k-fault combination if the meta-heuristic approach is used with a quantum computer size $Q = 1500$ according to (22). Reasonable selection of I is $I = 10$ for $k = 2, 3$, and $I = 100$ for $k = 4, 5$ as the probability to identify the worst-case contingency is above 90% assuming zero errors of annealer and Neumann approximation. This study shows the problem is decomposable but requires exponentially more samples, the more k-fault combinations are assessed. These results also show

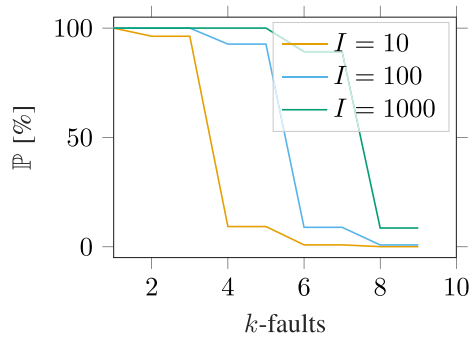

Fig. 12. Probability to assess k-faults when sampling I times and using a quantum computer with $Q = 1500$.

that the decomposition introduces the same limitation as in the conventional approach, the poor scaling to increasing k. In comparison, if the full problem fits on the annealer and the meta-heuristic approach is not needed, recap that the approach is feasible to process security assessment with constant computational times in k as Table V showed.

G. Discussion

We propose a novel 'backwards' process for security assessment that directly identifies the low-security contingency list, in contrast to state-of-the-art methods that exhaustively screen the entire contingency space. This fundamental shift leads to a remarkable improvement in computational efficiency. Our approach achieves an approximate $200\times$ speed-up for 50 faults in the IEEE 118-bus system, compared to exhaustive search methods. While the hardware used in our comparison differs, the results suggest that QA offers significant potential for addressing contingency analysis at scale. Our approach is the first to demonstrate constant computational complexity concerning common mode k-failures and concerning system size, to the best of our knowledge. When estimating the compute for the full system 187 possible faults (and all k combinations thereof), the state-of-the-art method takes around hours to days, and the QA may solve this problem within seconds to minutes. Using the QA distribution based on quantum effects may help identify lines to reinforce to withstand 'all' k faults.

There are several limitations of the QA-based approach, related to the power systems' validity and the scaling of the approach on currently available QA hardware. The currently applied security assessments assume the DC-approximation and assess only the overloading of transmission lines. Our approach can not provide insights into voltage issues, reactive power generation limits that would require an AC model. However, one could assess these security criteria with AC-models after the k-fault contingency list (the distribution) that has been obtained from the proposed approach, to further distinguish the criticality of these contingencies, part of the distribution. The limitations of the QA hardware impose limits on the number of lines and their combinations that can be included in the contingency list. As the system size grows, the number of required QUBOs increases approximately linearly with the number of lines in the network, i.e., testing each line for overload conditions requires solving at least two QUBOs per line. Although the meta-heuristic approach allows including more individual lines in the contingency list compared to a direct QA-based approach without heuristics, the meta-heuristic also requires even more QUBO solves, as each additional line or line-pair introduces further QUBOs. The time complexity of the search Algorithm 1 applying (16) is $\mathcal{O}(k|\Omega^L|)$ and assumes the full problem with all contingencies considered fits on a single QA. If the problem does not fit on a single QA, the time complexity of the heuristic Algorithm 2 is $\mathcal{O}(kI|\Omega^L|)$ with the user selecting I. The time complexity of an exhaustive search is $\mathcal{O}(|\Omega^L|^k)$. This research is an initial proof of concept and marks a first step towards QA-based N-k security assessment.

Improvements on the computation times are expected with better formulation of the problem, developing better meta-heuristics and larger QA hardware that the full problem fits on the QA. Improvements of the solution quality are expected with improvements in the quantum field, e.g. improving error mitigation (and handling) of the solutions obtained from the annealer. This specific QA-based approach can be further improved by tailoring the annealing process to this specific computational task. There, it is important to understand the relationship between the initial, mixing Hamiltonians and the initial state for QA [43]. The practical approach proposed does not scale well with the number of lines and combinations. The approach can likely be improved using other searches, like tabu. The disjunctive formulation would benefit from a reduction in auxiliary variables, as these require many additional qubits.

V. Conclusion

This research is a foundational, initial step toward enabling two novel use cases for power system security: to identify the most critical N-k contingency list in near real-time and determine the lines to reinforce to ensure system resilience against N-k faults. QA is promising for N-k security assessment due to the inherently combinatorial nature of the problem. Beyond N-k analysis, this research can inspire more use cases in (power) systems where combinatorial problems arise, specifically if one is interested in the distribution of solutions. From the case studies, we can conclude the proposed concept works for medium-sized power systems; however, the number of lines to consider faulty has to be limited (with all k combinations thereof). A speed-up of $200\times$ to exhaustive search was obtained when searching for critical k-contingencies. The meta-heuristic makes the problem feasible on currently available QA hardware, however introduces additional computations, e.g. the heuristic becomes impractical when focusing on $k > 4$ as many QUBOs would need to be solved. From the study on the IEEE 118-bus system, we conclude that lines for reinforcement can be identified by analysing the QA solution distribution. Therefore, future research should focus on problem formulations, reducing auxiliary variables, and more advanced practical approaches for current QA hardware.

Appendix A
Approximating Power Transfer Distribution Factors

This section provides background on approximating power transfer distribution factors (called polynomial LODFs in [24]). $A \in \{-1, 0, 1\}^{|\Omega^L| \times |\Omega^B|}$ is the branch incidence matrix. 1 and -1 represent the 'from bus' and 'to bus'. The susceptance matrix

is $B \in \mathbb{R}^{|\Omega^B|\times|\Omega^B|}$ with the elements

$$B_{\tilde{b},b} = \sum_{l\in\Omega^L} A_{l,b}A_{l,\tilde{b}}\frac{1}{\chi_l} \quad \forall b,\tilde{b}\in\Omega^B \tag{24a}$$

$$B_{b,b} = -\sum_{l\in\Omega^L} A_{l,b}A_{l,b}\frac{1}{\chi_l} \quad \forall b\in\Omega^B \tag{24b}$$

with line reactances χ_l. At the slack bus $\hat{b}$

$$B_{\hat{b},b} = 0 \quad \forall b\in\Omega^B$$

$$B_{b,\hat{b}} = 0 \quad \forall b\in\Omega^B \tag{25}$$

has zeros in the row and column. The power transfer distribution factors

$$PTDF = B_{br}\times A\times B^{-1}, \tag{26}$$

where $B_{br}\in\mathbb{R}^{|\Omega^L|\times|\Omega^L|}$ has the line reactance values in the diagonal entries, and all other elements are zero. B^{-1} is the Pseudoinverse. B_{br} and B are different matrices. If B alters from B to $B+D$ due to an outage d, the Woodbury identity [44] efficiently updates the inverse of the original matrix B changed by $D = U\mathcal{I}V$ by

$$(B+U\mathcal{I}V)^{-1} = B^{-1} - B^{-1}U(\mathcal{I}+VB^{-1}U)^{-1}VB^{-1}, \tag{27}$$

where $\mathcal{I}$ is the identity matrix with dimensions $|\Omega^B|\times|\Omega^B|$. The power transfer distribution factors are

$$PTDF_d = B_{br}\times A\times(B+U\mathcal{I}V)^{-1}, \tag{28}$$

with the matrix

$$U = \mathcal{I} + \sum_{l\in\Omega_d^{\hat{L}}} U_l \tag{29a}$$

$$U_l = -e_{b_l^t}e_{b_l^t}^T, \tag{29b}$$

where b_l^t is the 'to' bus, b_l^f is the 'from' bus of the line l. e_i is the standard basis vector where the ith element is one, and all other elements are zero. The matrix V is

$$V = \sum_{l\in\Omega_d^{\hat{L}}} V_l \tag{30a}$$

$$V_l = -\frac{1}{\chi_l}e_{b_l^f}e_{b_l^f}^T. \tag{30b}$$

A1 Polynomial Approximation of N-k PTDFs

The lines $\Omega_d^{\hat{L}}$ are in an outage at sample d and the matrix to invert to compute the $PTDF_d$ with (27)–(28) is

$$(\mathcal{I}+VB^{-1}U)^{-1} = (\mathcal{I}+\sum_{l\in\Omega_d^{\hat{L}}} V_lB^{-1}U)^{-1}. \tag{31}$$

We define

$$J_l := \mathcal{I} + V_lB^{-1}U, \tag{32a}$$

$$T_l := V_lB^{-1}U = V_lB^{-1}(\mathcal{I}+\sum_{\hat{l}\in\Omega_d^{\hat{L}}} U_{\hat{l}}) \tag{32b}$$

where $J_l = \mathcal{I}+T_l$. With (31)–(32), we obtain

$$(\mathcal{I}+VB^{-1}U)^{-1} = \left(J_l + \sum_{\hat{l}\in\Omega_d^{\hat{L}}\setminus l} T_{\hat{l}}\right)^{-1}. \tag{33}$$

We develop the Neumann series with one component around J_l

$$(\mathcal{I}+VB^{-1}U)^{-1} \approx J_l^{-1} \quad \forall l\in\Omega^{\hat{L}}, \tag{34}$$

which converges iff

$$\left\| J_l^{-1}\sum_{\hat{l}\in\Omega_d^{\hat{L}}\setminus l} T_{\hat{l}} \right\| < 1. \tag{35}$$

Then, we linearly combine all lines in the outage and subtract the identity $k-1$ times as each J has 1 entries on the diagonal.

$$(\mathcal{I}+VB^{-1}U)^{-1} \approx \sum_{l\in\Omega_d^{\hat{L}}} J_l^{-1} - (k-1)\mathcal{I}. \tag{36}$$

We then use (29a) and the distributive property to compute

$$J_l^{-1} = \left(\mathcal{I} + V_lB^{-1}\mathcal{I} + V_lB^{-1}U_l + \sum_{\hat{l}\in\Omega_d^{\hat{L}}\setminus l} V_lB^{-1}U_{\hat{l}}\right)^{-1}. \tag{37}$$

We define

$$E_l := \mathcal{I} + V_lB^{-1}\mathcal{I} + V_lB^{-1}U_l, \tag{38a}$$

$$R_l := \sum_{\hat{l}\in\Omega_d^{\hat{L}}\setminus l} V_lB^{-1}U_{\hat{l}} \tag{38b}$$

and expand with Neumann with one component around E_l, so

$$J_l^{-1} \approx E_l^{-1}, \tag{39}$$

which converges iff $||E_l^{-1}R_l|| < 1$. Then, the PTDFs are

$$(B+U\mathcal{I}V)^{-1} \approx B^{-1} - B^{-1}U\left(\sum_{l\in\Omega_d^{\hat{L}}} E_l^{-1} - (k-1)\mathcal{I}\right)VB^{-1}. \tag{40}$$

We use the distributed property to obtain

$$\begin{aligned}\tilde{B}^{-1} \approx B^{-1} &+ \sum_{l\in\Omega_d^{\hat{L}}} B^{-1}\mathcal{I}(\hat{k}-1)\mathcal{I}V_lB^{-1} \\ &+ \sum_{\hat{l}\in\Omega_d^{\hat{L}}}\sum_{l\in\Omega_d^{\hat{L}}} B^{-1}U_{\hat{l}}(\hat{k}-1)\mathcal{I}V_lB^{-1} \\ &- \sum_{\hat{l}\in\Omega_d^{\hat{L}}}\sum_{l\in\Omega_d^{\hat{L}}} B^{-1}\mathcal{I}E_l^{-1}V_{\hat{l}}B^{-1} \\ &- \sum_{\check{l}\in\Omega_d^{\hat{L}}}\sum_{\hat{l}\in\Omega_d^{\hat{L}}}\sum_{l\in\Omega_d^{\hat{L}}} B^{-1}U_{\check{l}}E_l^{-1}V_{\hat{l}}B^{-1}.\end{aligned} \tag{41}$$

REFERENCES

[1] F. Capitanescu, "Are we prepared against blackouts during the energy transition?: Probabilistic risk-based decision making encompassing jointly security and resilience," *IEEE Power Energy Mag.*, vol. 21, no. 3, pp. 77–86, MAy/Jun. 2023.

[2] R. Sarkar, "An analytical approach for reducing k-line failure analysis and load shed computation," *IET Gener., Transmiss. Distribution*, vol. 16, no. 13, pp. 2623–2641, 2022.

[3] K. Sundar, M. Vallem, R. Bent, N. Samaan, B. Vyakaranam, and Y. Makarov, "N-k failure analysis algorithm for identification of extreme events for cascading outage pre-screening process," in *Proc. IEEE Power Energy Soc. Gen. Meeting*, 2019, pp. 1–5.

[4] K. Köck, "Probability based transmission system risk assessment," Ph.D. dissertation, Graz Univ. Technol., Graz, Austria, Aug. 2016.

[5] E. Karangelos and L. Wehenkel, "Probabilistic reliability management approach and criteria for power system real-time operation," in *Proc. Power Syst. Computation Conf.*, Genoa, Italy, 2016, pp. 1–9.

[6] R. L.-Y. Chen, A. Cohn, N. Fan, and A. Pinar, "Contingency-risk informed power system design," *IEEE Trans. Power Syst.*, vol. 29, no. 5, pp. 2087–2096, 2014.

[7] D. S. Kirschen and D. Jayaweera, "Comparison of risk-based and deterministic security assessments," *IET Gener., Transmiss. Distrib.*, vol. 1, no. 4, pp. 527–533, 2007.

[8] B. N. Giraud, A. Rajaei, and J. L. Cremer, "Constraint-driven deep learning for N-k security constrained optimal power flow," *Electric Power Syst. Res.*, vol. 235, 2024, Art. no. 110692.

[9] P. Panciatici, G. Bareux, and L. Wehenkel, "Operating in the fog: Security management under uncertainty," *IEEE Power Energy Mag.*, vol. 10, no. 5, pp. 40–49, Sep./Oct. 2012.

[10] A. Abedi, L. Gaudard, and F. Romerio, "Power flow-based approaches to assess vulnerability, reliability, and contingency of the power systems: The benefits and limitations," *Rel. Eng. System Saf.*, vol. 201, 2020, Art. no. 106961.

[11] J. M. Arroyo and F. J. Fernández, "Application of a genetic algorithm to n-K power system security assessment," *Int. J. Elect. Power Energy Syst.*, vol. 49, pp. 114–121, 2013.

[12] T. Guler, G. Gross, and M. Liu, "Generalized line outage distribution factors," *IEEE Trans. Power Syst.*, vol. 22, no. 2, pp. 879–881, May 2007.

[13] A. J. Wood, B. F. Wollenberg, and G. B. Sheblé, *Power Generation, Operation, and Control*. Hoboken, NJ, USA: Wiley, 2013.

[14] V. Donde, V. Lopez, B. Lesieutre, A. Pinar, C. Yang, and J. Meza, "Severe multiple contingency screening in electric power systems," *IEEE Trans. Power Syst.*, vol. 23, no. 2, pp. 406–417, May 2008.

[15] C. M. Davis and T. J. Overbye, "Multiple element contingency screening," *IEEE Trans. Power Syst.*, vol. 26, no. 3, pp. 1294–1301, Aug. 2011.

[16] A. Pinar, J. Meza, V. Donde, and B. Lesieutre, "Optimization strategies for the vulnerability analysis of the electric power grid," *SIAM J. Optim.*, vol. 20, no. 4, pp. 1786–1810, 2010.

[17] S. Poudel, Z. Ni, and W. Sun, "Electrical distance approach for searching vulnerable branches during contingencies," *IEEE Trans. Smart Grid*, vol. 9, no. 4, pp. 3373–3382, Jul. 2018.

[18] K. Zhou, I. Dobson, and Z. Wang, "The most frequent N-k line outages occur in motifs that can improve contingency selection," *IEEE Trans. Power Syst.*, vol. 39, no. 1, pp. 1785–1796, Jan. 2024.

[19] T. V. Cutsem and T. Weckesser, "Searching for plausible N-k contingencies endangering voltage stability," in *Proc. IEEE PES Innov. Smart Grid Technol. Conf. Europe*, Turin, Italy, 2017, pp. 1–6.

[20] J. L. Cremer and G. Strbac, "A machine-learning based probabilistic perspective on dynamic security assessment," *Int. J. Elect. Power Energy Syst.*, vol. 128, 2021, Art. no. 106571.

[21] Y. Liu, N. Zhang, D. Wu, A. Botterud, R. Yao, and C. Kang, "Searching for critical power system cascading failures with graph convolutional network," *IEEE Trans. Control Netw. Syst.*, vol. 8, no. 3, pp. 1304–1313, Sep. 2021.

[22] T. Ding, C. Li, C. Yan, F. Li, and Z. Bie, "A bilevel optimization model for risk assessment and contingency ranking in transmission system reliability evaluation," *IEEE Trans. Power Syst.*, vol. 32, no. 5, pp. 3803–3813, Sep. 2017.

[23] J. McCalley et al., "Probabilistic security assessment for power system operations," in *Proc. IEEE Power Eng. Soc. Gen. Meeting*, Denver, CO, USA, 2004, vol. 1, pp. 212–220.

[24] J. L. Cremer, "Polynomial line outage distribution factors for estimating expected congestion and security," *IEEE Trans. Power Syst.*, vol. 40, no. 3, pp. 2532–2544, May 2025.

[25] M. A. Ortega-Vazquez, "Assessment of N-k contingencies in a probabilistic security-constrained optimal power flow," in *Proc. IEEE Power Energy Soc. Gen. Meeting*, 2016, pp. 1–5.

[26] L. Huang, C. S. Lai, Z. Zhao, G. Yang, B. Zhong, and L. L. Lai, "Robust $N-k$ security-constrained optimal power flow incorporating preventive and corrective generation dispatch to improve power system reliability," *CSEE J. Power Energy Syst.*, vol. 9, no. 1, pp. 351–364, Jan. 2023.

[27] R. Eskandarpour, K. J. B. Ghosh, A. Khodaei, A. Paaso, and L. Zhang, "Quantum-enhanced grid of the future: A primer," *IEEE Access*, vol. 8, pp. 188993–189002, 2020.

[28] Y. Zhou et al., "Quantum computing in power systems," *iEnergy*, vol. 1, no. 2, pp. 170–187, Jun. 2022.

[29] F. Feng, Y. Zhou, and P. Zhang, "Quantum power flow," *IEEE Trans. Power Syst.*, vol. 36, no. 4, pp. 3810–3812, Jul. 2021.

[30] B. Sævarsson, S. Chatzivasileiadis, H. Jóhannsson, and J. Østergaard, "Quantum computing for power flow algorithms: Testing on real quantum computers," in *Proc. 11th Bulk Power Syst. Dyn. Control Symp.*, Banff, AB, Canada, 2022 [Online]. Available: https://arxiv.org/abs/2204.14028.

[31] R. Eskandarpour, P. Gokhale, A. Khodaei, F. T. Chong, A. Passo, and S. Bahramirad, "Quantum computing for enhancing grid security," *IEEE Trans. Power Syst.*, vol. 35, no. 5, pp. 4135–4137, Sep. 2020.

[32] N. Nikmehr and P. Zhang, "Quantum-inspired power system reliability assessment," *IEEE Trans. Power Syst.*, vol. 38, no. 4, pp. 3476–3490, Jun. 2023.

[33] S. A. Hosseini, A. Monti, and S. Peyghami, "Modern power system risk assessment using quantum computing," in *Proc. 18th Int. Conf. Probabilistic Methods Appl. Power Syst.*, Auckland, New Zealand, 2024, pp. 1–6.

[34] H. Yang, Y. Liu, Y. Yue, D. Zhang, and Y. Ma, "Power system reliability assessment technique and modeling approach based on quantum computing theory," *Electric Power Syst. Res.*, vol. 236, 2024, Art. no. 110957.

[35] T. T. Tran et al., "A hybrid quantum-classical approach to solving scheduling problems," in *Proc. 9th Annu. Symp. Combinatorial Search*, J. A. Baier and A. Botea, Eds., Tarrytown, NY, USA, Jul. 2016, pp. 98–106.

[36] T. Morstyn, "Annealing-based quantum computing for combinatorial optimal power flow," *IEEE Trans. Smart Grid*, vol. 14, no. 2, pp. 1093–1102, Mar. 2023.

[37] Z. Kaseb, M. Möller, P. P. Vergara, and P. Palensky, "Power flow analysis using quantum and digital annealers: A discrete combinatorial optimization approach," *Sci. Rep.*, vol. 14, no. 1, Oct. 2024, Art. no. 23216.

[38] R. Eskandarpour, K. Ghosh, A. Khodaei, and A. Paaso, "Experimental quantum computing to solve network DC power flow problem," in *Proc. CIGRE Grid Future Symp.*, Providence, RI, USA, Oct. 2021.

[39] F. Glover, G. Kochenberger, R. Hennig, and Y. Du, "Quantum bridge analytics I: A tutorial on formulating and using QUBO models," *Ann. Operations Res.*, vol. 314, no. 1, pp. 141–183, Jul. 2022.

[40] P. Pareek, A. Jayakumar, C. Coffrin, and S. Misra, "Limitations of fault-tolerant quantum linear system solvers for quantum power flow," *IEEE Transactions on Power Systems*, pp. 1–10, 2025. doi:10.1109/TPWRS.2025.3613139.

[41] B. Xiong, D. Fioriti, F. Neumann, I. Riepin, and T. Brown, "Modelling the high-voltage grid using open data for Europe and beyond," *Sci. Data*, vol. 12, no. 1, Feb. 2025, Art. no. 277.

[42] A. Verma, M. Lewis, and G. Kochenberger, "Efficient QUBO transformation for higher degree pseudo Boolean functions," 2021, *arXiv:2107.11695*.

[43] B. Yan and N. A. Sinitsyn, "Analytical solution for nonadiabatic quantum annealing to arbitrary Ising spin Hamiltonian," *Nature Commun.*, vol. 13, no. 1, 2022, Art. no. 2212.

[44] M. A. Woodbury, "Inverting modified matrices," Statistical Research Group, Princeton University, Princeton. NJ, Memorandum Report 42, 1950.